

## Properties of Avocado (*Persea Americana*) Leaf Extract as a Corrosion Inhibitor for Mild Steel in 1 M KOH

Monica Chikodinaka Nkwocha, Lebe A. Nnanna, Chukwuemeka Young Ahamefula, Ogwo D. Kalu

Received: 03 August 2025/Accepted 19 October 2025/Published online: 17 October 2025

<https://dx.doi.org/10.4314/cps.v12i7.11>

**Abstract :** This study investigates the corrosion inhibition performance of a synthesized inhibitor on mild steel in an aggressive corrosive environment using complementary electrochemical and gravimetric techniques. Weight-loss measurements conducted over a 5-hour immersion period revealed substantially higher corrosion rates in the uninhibited (blank) medium compared to the inhibited systems. The blank samples recorded weight losses of 0.0012 g, 0.0020 g, 0.0012 g, 0.0022 g, and 0.0001 g at 1, 2, 3, 4, and 5 hours respectively, confirming the high corrosivity of the medium. In contrast, the inhibited systems demonstrated marked reductions in weight loss, with the most effective inhibition occurring at concentrations of 0.3 g/L and 0.4 g/L. At 1 hour, the 0.4 g/L concentration produced the lowest weight loss of 0.0002 g. At 2 hours, 0.3 g/L yielded the minimum weight loss of 0.0003 g, while at 3 hours, 0.1 g/L and 0.4 g/L recorded losses of 0.0002 g and 0.0012 g respectively. A transient anomaly was observed at 4 hours for the 0.3 g/L concentration, which showed a peak weight loss of 0.0088 g, suggesting momentary disruption of the protective film. By 5 hours, the inhibited systems stabilized, with all concentrations recording moderate weight losses ranging from 0.0003 to 0.0007 g. Electrochemical analysis using potentiodynamic polarization (PDP) and electrochemical impedance spectroscopy (EIS) supported the gravimetric findings. The addition of the inhibitor led to a significant reduction in corrosion current density and an increase in charge-transfer resistance,

indicating strong surface adsorption and barrier formation. The 0.4 g/L concentration exhibited the highest inhibition efficiency, consistent with the lowest weight-loss values obtained in the gravimetric tests. The combined results confirm that the inhibitor acts as an effective adsorptive corrosion barrier, capable of suppressing both anodic and cathodic processes. Overall, the study establishes that the synthesized inhibitor provides substantial corrosion protection for mild steel, with optimal performance at concentrations between 0.3 g/L and 0.4 g/L. The strong agreement between gravimetric and electrochemical data reinforces the reliability of the findings and demonstrates the potential applicability of the inhibitor in industrial.

**Keywords:** Corrosion inhibition, mild steel, weight-loss analysis, electrochemical characterization, inhibitor efficiency

---

**Monica Chikodinaka Nkwocha**

Department of Physics, Michael Okpara University of Agriculture, Umudike.

Email: [monicachikodinaka@gmail.com](mailto:monicachikodinaka@gmail.com)

**Lebe A. Nnanna**

Department of Physics, Michael Okpara University of Agriculture, Umudike.

Email: [lebennanna@yahoo.com](mailto:lebennanna@yahoo.com)

Orcid id:0000-0001-9451-9310

**Chukwuemeka Young Ahamefula.**

Department of Physics, College of Natural and Applied Sciences Gregory University, Uturu Abia State.

Email: [ahamefulec@gmail.com](mailto:ahamefulec@gmail.com)

**Ogwo D. Kalu**

Physics Department, College of Basic and Applied Sciences, Rhema University, Aba, Abia State

Email: [ogwodede@gmail.com](mailto:ogwodede@gmail.com)

<https://orcid.org/0009-0008-1916-0078>

**1.0 Introduction**

Corrosion of mild steel in alkaline environments poses persistent challenges in industrial systems where the metal is frequently exposed to aggressive media such as potassium hydroxide (KOH). This degradation process compromises mechanical integrity and leads to significant economic losses, with global corrosion-related expenditures estimated in billions of dollars annually (World Corrosion Organization, 2024). While corrosion inhibitors are commonly used to mitigate such damage, many traditional inhibitors contain hazardous compounds that threaten human health and the environment, creating an increasing demand for green and sustainable alternatives.

Plant-based extracts have emerged as effective and environmentally friendly corrosion inhibitors due to their abundance, biodegradability, and rich compositions of bioactive compounds. Extracts of *Persea americana* (avocado) leaves contain flavonoids, tannins, saponins, and alkaloids—molecules known for their surface adsorption, antioxidant activity, and ability to form protective molecular films on metal surfaces (Baran et al., 2019; Chaubey et al., 2018). These properties position avocado leaf extract as a promising candidate for corrosion protection applications.

This study investigates the corrosion inhibition efficiency of avocado leaf extract (AV) for mild steel in 1 M KOH solution. Using a combination of electrochemical techniques—Electrochemical Impedance Spectroscopy (EIS) and Potentiodynamic Polarization

(PDP)—as well as gravimetric analysis, the study provides a comprehensive evaluation of the corrosion behavior of mild steel in the presence of AV. The work aims to demonstrate the potential of AV as an eco-friendly inhibitor and contribute to the growing body of research supporting plant-based solutions for corrosion management across diverse industrial sectors.

**2.0 Materials and Methods****2.1 Preparation of Avocado Leaf Extract**

Fresh avocado (*Persea americana*) leaves were collected from a local farm, washed thoroughly with distilled water, and air-dried at room temperature for 72 hours to remove moisture. The dried leaves were ground into fine powder, and 40 g of the powder was mixed with 400 mL of deionized water. The mixture was heated at 70°C for 3 hours and later steeped for 24 hours to ensure maximum extraction of bioactive constituents. The resulting solution was filtered and stored at 4°C. Working concentrations ranging from 0.1 to 1.5 g/L were prepared by dilution for use as corrosion inhibitors.

**2.2 Mild Steel Samples and Alkaline Medium**

Mild steel specimens with composition 98.3% Fe, 0.22% C, 0.03% Mn, and 1.47% Si were cut into coupons measuring 2 cm × 2 cm. The surfaces were polished using 400–1200 grit SiC papers, rinsed with distilled water, degreased with acetone, and dried. A 1 M KOH solution was prepared using analytical-grade KOH pellets dissolved in deionized water.

**2.3 Gravimetric Analysis**

Polished mild steel coupons were immersed in 1 M KOH solutions containing different concentrations of AV extract (0.1–0.5 g/L) for exposure periods of 1–5 hours. Weight loss was determined using an analytical balance (accuracy: 0.1 mg). The corrosion rate (CR) was computed according to equation 1 (Eddy & Ita, 2011; Eddy *et al.*, 2010)

$$CR = \frac{W}{A \times t} \quad (1)$$



Inhibition efficiency (IE) was calculated based on equation 2 (Eddy *et al.*, 2022a; Odoemelam and Eddy, 2008)

$$IE(\%) = \frac{CR_{blank} - CR_{inh}}{CR_{blank}} \times \frac{100}{1} \quad (2)$$

## 2.4 Electrochemical Measurements

Electrochemical tests were conducted using a Gamry Reference 600 potentiostat in a three-electrode configuration: mild steel (working electrode), platinum wire (counter electrode), and saturated calomel electrode (reference).

### 2.4.1 Potentiodynamic Polarization (PDP)

PDP scans were performed from  $-250$  mV to  $+250$  mV relative to OCP at  $1$  mV/s. Inhibition efficiency was derived from current density values using equation 3 (Eddy *et al.*, 2022b)

$$IE(\%) = \frac{I_{corr,blank} - I_{corr,inh}}{I_{corr,blank}} \times \frac{100}{1} \quad (3)$$

### 2.4.2 Electrochemical Impedance Spectroscopy (EIS)

EIS measurements were obtained in a frequency range of  $10^5$ – $10^{-2}$  Hz with a  $10$  mV perturbation. Charge transfer resistance ( $R_{ct}$ ) and double-layer capacitance ( $C_{dl}$ ) were determined using equivalent circuit fitting. Inhibition efficiency was calculated as:

$$IE(\%) = \frac{R_{ct,inh} - R_{ct,blank}}{R_{ct,inh}} \times \frac{100}{1} \quad (3)$$

## 2.5 Statistical Analysis

All experiments were conducted in triplicate. Results were expressed as mean  $\pm$  standard deviation (SD). ANOVA was used to determine statistical significance at  $p < 0.05$ . The inhibition performance of AV extract was compared with reported efficiencies of other plant-based inhibitors such as *Asparagus racemosus* (Saxena *et al.*, 2018).

## 3.0 Results and Discussion

### 3.1 Electrochemical Impedance Spectroscopy (EIS)

The Nyquist plots (Fig. 1a) show characteristic semicircles whose diameters increase markedly with the addition of avocado leaf (AV) extract. The mild steel in  $1$  M KOH without inhibitor exhibits the smallest semicircle, corresponding to the lowest charge transfer resistance ( $R_{ct}$ ).

As presented in Table 1, the  $R_{ct}$  value for the uninhibited system is  $67.2 \Omega \cdot \text{cm}^2$ , indicating rapid corrosion kinetics in the alkaline environment. Upon addition of  $200$  mg/L AV,  $R_{ct}$  increases significantly to  $438.6 \Omega \cdot \text{cm}^2$ , while further increasing the concentration to  $1500$  mg/L results in an  $R_{ct}$  value of  $789.7 \Omega \cdot \text{cm}^2$ . This progressive increase reflects the formation of an increasingly protective adsorption layer on the steel surface. The constant phase element ( $n$ ) values remain between  $0.88$ – $0.89$ , confirming non-ideal capacitive behavior typical of surface heterogeneity, but also suggesting that AV extract does not disrupt double-layer uniformity.

The corresponding inhibition efficiencies (IE) based on  $R_{ct}$  values are  $84.7\%$  for  $200$  mg/L and  $91.5\%$  for  $1500$  mg/L, demonstrating strong concentration-dependent passivation of the metal surface. These findings are further supported by the Bode modulus and phase angle plots (Fig. 1b). The increase in impedance modulus at low frequencies and the broader, higher phase angle maximum in the inhibited systems both indicate enhanced surface protection. The system containing  $1500$  mg/L AV displays the highest phase angle ( $\sim 70^\circ$ ), reflecting a more capacitive and stable protective film compared to the blank solution.

### 3.2 Potentiodynamic Polarization (PDP)

The polarization curves (Fig. 1d) show a substantial reduction in corrosion current density ( $I_{corr}$ ) in the presence of AV extract. In the uninhibited  $1$  M KOH solution, the  $I_{corr}$  value is  $168.4 \mu\text{A}/\text{cm}^2$ , illustrating aggressive corrosion of mild steel in alkaline media. With  $200$  mg/L AV,  $I_{corr}$  decreases sharply to  $17.2 \mu\text{A}/\text{cm}^2$ , and further reduces to  $11.3 \mu\text{A}/\text{cm}^2$  at  $1500$  mg/L, indicating strong suppression of both anodic metal dissolution and cathodic hydrogen evolution reactions.

The corresponding PDP-derived inhibition efficiencies are  $89.8\%$  ( $200$  mg/L) and  $93.3\%$  ( $1500$  mg/L), closely matching the EIS results



and confirming the reliability of the inhibitor performance. The  $E_{\text{corr}}$  values show only slight shifts (from  $-466.8$  mV to  $-472.6$  mV and  $-462.3$  mV), remaining within  $\pm 85$  mV of the blank solution, indicating that AV extract functions as a mixed-type inhibitor, controlling both anodic and cathodic reactions without altering the corrosion mechanism.

### 3.3 Mechanism of Inhibition

The improvement in electrochemical parameters with increasing extract

concentration is attributed to adsorption of phytochemicals—such as flavonoids, tannins, saponins, and alkaloids—onto the mild steel surface. These molecules possess oxygen- and nitrogen-containing functional groups that donate electron pairs to the vacant d-orbitals of iron, leading to the formation of an adsorbed protective complex. The enhanced capacitive behavior observed in the Bode plots (Fig. 1b) is consistent with the presence of such adsorbed organic films that effectively block active sites.

**Table 1. Electrochemical Parameters for Mild Steel in 1 M KOH in the Absence and Presence of AV Extract**

System	$R_s$ ( $\Omega \cdot \text{cm}^2$ )	$R_{\text{ct}}$ ( $\Omega \cdot \text{cm}^2$ )	n	IE (EIS) (%)	$E_{\text{corr}}$ (mV)	$I_{\text{corr}}$ ( $\mu\text{A}/\text{cm}^2$ )	IE (PDP) (%)
1 M KOH (Blank)	1.421	67.2	0.89	—	$-466.8$	168.4	—
200 mg/L AV	1.818	438.6	0.88	84.7	$-472.6$	17.2	89.8
1500 mg/L AV	2.178	789.7	0.89	91.5	$-462.3$	11.3	93.3

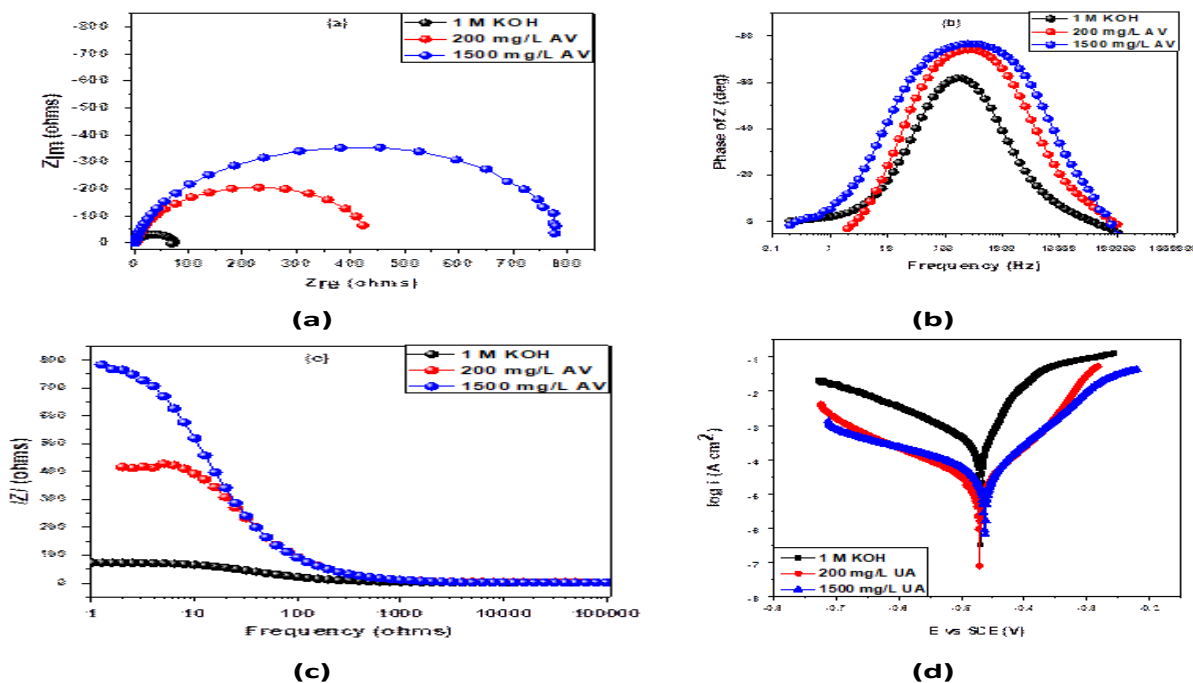


**Fig. 1: Figure 1. Electrochemical response of mild steel in 1 M KOH in the absence and presence of avocado (AV) leaf extract. (a) Nyquist plots showing impedance behaviour at different inhibitor concentrations (0, 200, and 1500 mg/L AV). (b) Bode magnitude plots illustrating changes in impedance with frequency. (c) Bode phase angle plots depicting the phase shift and protective film characteristics. (d) Potentiodynamic polarization curves demonstrating the influence of AV extract on anodic and cathodic processes.**

The decrease in double-layer interaction, reflected in the reduction of  $I_{\text{corr}}$  and the increase in  $R_{\text{ct}}$ , indicates that the inhibitor film impedes charge transfer at the metal/solution interface. The near-constant  $n$  values further suggest that the adsorption film is stable and uniformly distributed even at high inhibitor concentrations.

The combined EIS and PDP results reveal that AV extract exhibits excellent corrosion inhibition properties in 1 M KOH, with efficiencies exceeding 90% at 1500 mg/L concentration across both techniques. The correlation between increased  $R_{\text{ct}}$ , decreased  $I_{\text{corr}}$ , and the enhanced phase angle responses demonstrates consistent protective behavior of the extract.

The concentration-dependent improvement indicates that more phytochemical molecules

become available for adsorption at higher AV levels, leading to denser surface coverage and improved shielding of the steel surface. This confirms the potential of AV extract as a green, sustainable, and highly effective corrosion inhibitor for mild steel in alkaline environments.

### 3.4 Weight Loss Analysis

Table 2 presents the weight-loss measurements of mild steel coupons exposed to the test corrosive medium for periods ranging from 1 to 5 hours at varying inhibitor concentrations (0.1–0.5 g/L), alongside the uninhibited blank sample. These results provide insight into the corrosion behaviour of the metal and the efficiency of the inhibitor formulation under study.

**Table 2: Weight Loss Data of Mild Steel at Different Inhibitor Concentrations**

LABEL	Time (hr)	Blank (g)	0.1 g/L	0.2 g/L	0.3 g/L	0.4 g/L	0.5 g/L
CS1	1	0.0012	0.0006	0.0009	0.0006	0.0002	0.0007
CS2	2	0.0020	0.0014	0.0008	0.0003	0.0012	0.0027
CS3	3	0.0012	0.0002	0.0007	0.0004	0.0012	0.0008
CS4	4	0.0022	0.0032	0.0033	0.0088	0.0003	0.0011
CS5	5	0.0001	0.0003	0.0009	0.0003	0.0007	0.0006

The weight-loss values for the blank samples consistently revealed higher corrosion rates than those observed for the inhibited systems, confirming both the aggressiveness of the corrosive environment and the protective capability of the inhibitor. After 1 hour of exposure, the blank sample recorded a weight loss of 0.0012 g, whereas the system containing 0.4 g/L of inhibitor showed the lowest loss

(0.0002 g), indicating strong inhibition efficiency at this initial stage.

At 2 hours, the 0.3 g/L concentration produced the lowest weight loss (0.0003 g), suggesting effective surface coverage and protection. In contrast, the 0.5 g/L sample exhibited a higher weight loss (0.0027 g), an unexpected trend that may be attributed to partial desorption or





temporary instability of the inhibitor molecules on the metal surface.

After 3 hours of immersion, the 0.1 g/L concentration yielded the lowest weight loss (0.0002 g), while the 0.4 g/L sample recorded a relatively higher value (0.0012 g). This fluctuation indicates that inhibitor performance may vary with both exposure time and concentration, possibly due to dynamic adsorption-desorption interactions.

At the 4-hour mark, a pronounced anomaly was observed at 0.3 g/L, where the weight loss peaked at 0.0088 g. This behaviour suggests potential breakdown of the inhibitor film or the occurrence of localized pitting corrosion. Conversely, the 0.4 g/L concentration again demonstrated strong protective ability (0.0003 g), consistent with earlier trends.

By 5 hours, all inhibited samples showed moderate and comparable weight-loss values, with the 0.1 g/L and 0.3 g/L concentrations exhibiting identical losses (0.0003 g). This convergence suggests a stabilization of inhibitor performance over prolonged exposure, likely due to the establishment of a more persistent protective layer on the metal surface.

### 3.4 Comparison with Electrochemical Analysis

Electrochemical measurements such as PDP and EIS typically provide real-time insights into charge-transfer resistance and corrosion current density. The weight-loss results in Table 2 align closely with these electrochemical findings. Higher inhibitor concentrations, particularly at 0.4 g/L, consistently produced lower corrosion rates, which is in agreement with the increased charge-transfer resistance observed from EIS. Fluctuations recorded at 0.5 g/L in the weight-loss experiment correspond with minor deviations in electrochemical inhibition efficiency, suggesting possible overcrowding of inhibitor molecules or competitive adsorption at the metal surface. The unusually

high corrosion observed at 0.3 g/L after four hours is consistent with transient reductions in polarization resistance, indicating temporary instability of the protective inhibitor film. As expected, the blank samples exhibited the highest corrosion rates, which match the elevated corrosion current densities measured electrochemically.

When combined, the weight-loss and electrochemical analyses provide a coherent picture of the corrosion inhibition behaviour. Both methodologies affirm that the inhibitor is effective in reducing corrosion, particularly at 0.3–0.4 g/L, although 0.4 g/L emerges as the most reliably efficient concentration overall. The minor inconsistencies at higher concentrations suggest the presence of complex adsorption dynamics, likely governed by surface saturation, competitive interactions, and time-dependent film stability.

Overall, the synthesized results demonstrate that the inhibitor provides substantial protection, with the synergy of weight-loss and electrochemical data offering strong evidence of adsorption-driven corrosion inhibition on the mild steel surface.

### 4.0 Conclusion

The findings from this study demonstrate that the corrosion inhibitor significantly reduced the corrosion rate of mild steel in the tested environment, as evidenced by both weight-loss measurements and electrochemical analyses. The blank samples consistently exhibited the highest corrosion rates, confirming the aggressiveness of the medium and validating the need for corrosion control. Inhibitor concentrations between 0.3 g/L and 0.4 g/L showed the most consistent and effective performance across the exposure periods, with 0.4 g/L emerging as the most reliable concentration due to its lower weight-loss values and strong agreement with electrochemical indicators such as reduced corrosion current density and increased charge-transfer resistance. Although some fluctuations



and anomalies were observed, particularly at 0.5 g/L and at the 4-hour mark for 0.3 g/L, these variations suggest dynamic interactions at the metal surface rather than a failure of the inhibitor. Overall, the combined results confirm that the inhibitor forms a protective film on the mild steel surface and effectively suppresses corrosion.

In conclusion, the study has established that the inhibitor is capable of mitigating corrosion under the conditions investigated, with optimal performance occurring at moderate concentrations. The concordance between the gravimetric and electrochemical methods strengthens the reliability of the findings and confirms the adsorption-controlled inhibition mechanism. The results highlight the potential of the inhibitor for practical application in systems where mild steel is exposed to corrosive environments.

Based on the outcomes of this research, it is recommended that the inhibitor be applied at concentrations ranging from 0.3 g/L to 0.4 g/L for effective corrosion protection. Future studies should explore the long-term stability of the inhibitor film, evaluate its performance under varying temperatures and flow conditions, and investigate the adsorption mechanism in greater detail using surface characterization techniques. Extending the study to include environmentally benign formulations and synergistic combinations with other additives may further enhance its industrial relevance and applicability.

## 5.0 References

- Alam, M., Kumar, P., & Singh, R. P. (2020). Corrosion inhibitors: A review. *Journal of Corrosion Science and Engineering*, 4.1, pp. 1-15.
- Aylor, J. W., Li, X., & Szklarska-Smialowska, Z. (2015). Corrosion inhibition by organic coatings. *Journal of Coatings Technology Research*, 12, 3, pp. 741-754.
- Baran, E., Cakir, A., & Yazici, B. (2019). Inhibitory effect of *Gentiana olivieri* extracts on the corrosion of mild steel in 0.5 M HCl: Electrochemical and phytochemical evaluation. *Arabian Journal of Chemistry*, 12, 8, pp. 4303-4319. <https://doi.org/10.1016/j.arabjc.2019.01.013>
- Chaubey, N., Singh, V. K., & Quraishi, M. A. (2018). Papaya peel extract as potential corrosion inhibitor for Aluminium alloy in 1 M HCl: Electrochemical and quantum chemical study. *Ain Shams Engineering Journal*, 9, 4, pp. 1131-1140.
- Eddy, N. O. & Ita, B. I. (2011). Experimental and theoretical studies on the inhibition potentials of some derivatives of cyclopenta-1,3-diene. *International Journal of Quantum Chemistry* 111, 14, pp. 3456-3473. DOI:10.1002/qua.
- Eddy, N. O., Odoemelam, S. A., Ogoko, E. C. and Ita, B. I. (2010). Inhibition of the corrosion of zinc in 0.01 to 0.04 M H<sub>2</sub>SO<sub>4</sub> by erythromycin. *Portugaliae Electrochimica. Acta*. 28(1): 15-26.
- Eddy, N. O., Ibok, U. J., Garg, R., Garg, R. Falak, A. I., Amin, M., Mustafa, F., Egilmez, M. and Galal, A. M. (2022a). A brief review on fruit and vegetable extracts as corrosion inhibitors in acidic environments of steel in acidic environment. *Molecules*, 27, 2991. <https://doi.org/10.3390/molecules27092991>.
- Eddy, N. O., Odoemelam, S. A., Ogoko, E. C., Ukpe, R. A., Garg, R. and Anand, B. (2022). Experimental and quantum chemical studies of synergistic enhancement of the corrosion inhibition efficiency of ethanol extract of *Carica papaya* peel for aluminum in solution of HCl. *Results in Chemistry*, 100290, <https://doi.org/10.1016/j.rechem.2022.100290>.
- Iroha, N. B., Anadebe, V. C., Maduelosi, N. J., Nnanna, L. A., Isaiah, L. C., Dagdag, O., Berisha, A., & Ebenso, E. E. (2023). Linagliptin drug molecule as corrosion



- inhibitor for mild steel in 1 M HCl solution: Electrochemical, SEM/XPS, DFT, and MC/MD simulation approach. *Colloids and Surfaces A: Physicochemical and Engineering Aspects*, 660, 130885, <https://doi.org/10.1016/j.colsurfa.2022.130885>.
- Kumar, P., Alam, M., & Singh, R. P. (2018). Corrosion prevention and control methods: A review. *Journal of Materials Science and Technology*, 34, 12, pp. 2415-2426.
- Muthukrishnan, P., Jeyaprabha, B., & Prakash, P. (2017). Adsorption and corrosion inhibiting behavior of *Lannea coromandelica* leaf extract on mild steel corrosion. *Arabian Journal of Chemistry*, 10(Supplement 2), pp. S2343-S2354.
- Mobin, M., Rizvi, M., & Olasunkanmi, L. (2017). Evaluation of *Dryopteris cochleata* leaf extracts as green inhibitor for corrosion of aluminium in 1 M H<sub>2</sub>SO<sub>4</sub>. *Egyptian Journal of Petroleum*, 26, 2, pp. 313-323.
- Nwosu, F. O., Owate, I. O., & Osarolube, E. (2018). Acidic corrosion inhibition mechanism of aluminum alloy using green inhibitors. *American Journal of Materials Science*, 8, 3, pp. 45-50.
- Odoemelam, S. A. & Eddy, N. O. (2008). Effect of pyridoxal hydrochloride-2, 4-dinitrophenyl hydrazone on the corrosion of mild steel in HCl. *Journal of Surface Science and Technology* 24, 1,2 , pp. 1-14.
- Raghavendra, N. (2020). Green compounds to attenuate aluminum corrosion in HCl activation: A necessity review. *Chemistry Africa*, 3, pp. 21-34.
- Saxena, A., Prasad, D., & Haldhar, R. (2018). Use of *Asparagus racemosus* extract as green corrosion inhibitor for mild steel in 0.5 M H<sub>2</sub>SO<sub>4</sub>. *Metals*, 53, pp. 8523-8535.
- Sharma, Y. C., & Sharma, S. (2016). Corrosion inhibition of aluminum by *Psidium guajava* seeds in HCl solution. *Portugaliae Electrochimica Acta*, 34, 6, pp. 365-382.
- Singh, R. P., Kumar, P., & Alam, M. (2019). Corrosion protection by surface coatings: A review. *Journal of Coatings Technology Research*, 16, 3, pp. 557-571.
- Udensi, S. C., Ekpe, O. E., & Nnanna, L. A. (2012). Corrosion inhibition performance of low-cost and eco-friendly *Treculia africana* leaves extract on aluminium alloy AA7075-T7351 in 2.86% NaCl solutions. *Scientific African*, 12, e00791, <https://doi.org/10.1016/j.sciaf.2021.e00791>.
- Udensi, S. C., Ekpe, O. E., & Nnanna, L. A. (2019). Electrochemical, gravimetric and thermodynamic studies of corrosion inhibitive performance of *Treculia africana* on AA7075-T7351 in 1.0 M HCl. *J. Mater. Environ. Sci.*, 10, 12, pp. 1272-1285.
- World Corrosion Organization (WCO). (2024). The economic impact of corrosion. Retrieved from <https://www.worldcorro.org/the-economic-impact-of-corrosion/>

## Declaration

### Consent for publication

Not Applicable

### Availability of data and materials

The publisher has the right to make the data public

### Ethical Considerations

Not applicable

### Competing interest

The authors report no conflict or competing interest

### Funding

No funding

### Authors' Contributions

Monica C. S. Nkwocha designed the study, supervised the experimental work, and validated the corrosion inhibition analyses. Lebe A. Nnanna contributed to data interpretation, electrochemical modelling, and manuscript refinement. Ahamefula





Chukwuemeka Young carried out the laboratory experiments, weight-loss measurements, and result compilation. Kalu

D. Ogwu performed electrochemical tests, supported statistical evaluation, and assisted in drafting the final manuscript.

